Static and Vibrational FEM Analysis to develop an Improved U-2 Wing

J. Dickson
School of Engineering, RMIT University
S3719855@student.rmit.edu.au

ABSTRACT: Explored is the potential of Finite Element Analysis (FEM) technology like Abacus CAE to reduce the time and increase the effectiveness when prototyping an aircraft wing. Specifically, those found on the U-2 Dragon Lady. Several materials and airfoils are chosen, and FEM techniques are used to evaluate their performance. It is found that FEM does dramatically speed up the prototyping phase and serves to be a valuable tool for refinement and validation.

KEY WORDS: *FEM, Wing Structures, Weight Reduction*

Introduction

Considered is the place of Finite Element Analysis techniques in the refinement of an aircraft wing. Specifically, the U-2 Dragon Lady. This report intends to explore the use of this technology on weight reduction and vibration analysis regarding aircraft wings. We will take an assortment of airfoils and materials and use FEM to evaluate these and assess where we could refine these designs.

Section Schematics

In this section the schematics for two airfoils; the NACA 2412 and NACA 4412.

FIGURE A: NACA 2412 Airfoil

FIGURE B: NACA 4412 Airfoil

Both airfoils have a chord length of 3m and a skin thickness of 10mm. These sections were chosen using lift coefficient data and assessing the lifting viability based on this data (see Appendix C). A single wings total span is 14m. With a total aircraft span of 28m. For this report 14m single wing spans are considered.

Material Properties

TABLE A: A summary of the materials and their relevant properties. In SI Units (see Appendix A).

Props	*Aluminum 7075-T6*	*SAE 304 Stainless Steel*
Density	2810	7900
Youngs	71.7	193
Poisson's	0.33	0.3
Yield Stress	430	215

These materials were chosen as potential wing materials. The Aluminum has considerable weight benefits due to density. The steel however is much less elastic and so has high deformation resistance.

Weights and loading conditions

TABLE B: A summary of the wing weight and the loading conditions for each case. In SI Units (see Appendix B).

Airfoil	*2412*		*4412*	
Material	304	7075	304	7075
Mass	6775	2410	6796	2417
Wing Weight	66462	23642	66668	23710
Fuel Weight	53400	53400	53400	53400
Lift Force	112638	112638	155459	155459

The fuel weight is placed as a concentrated load at 400mm along the beam from the root, similarly an inertial mass is also applied at this point for vibrational analysis.

Regarding lift, a line force is applied across the entire beam when relevant.

The wing weight is simulated with a gravity force for the whole body. This is then determined through an Abacus CAE query of the mass properties.

The wing is fully constrained at the root and cannot move in any of the 6 degrees of freedom.

The beam is modeled as a cubic 3D beam (B33).

A beam profile that represents the relevant NACA Airfoil is applied and so allows Abacus CAE to determine the relevant bending and mass properties.

Results

Static Analysis

Using Abacus CAE each beam could be modeled and analyzed. We applied the relevant loading conditions as outlined in the previous sections.

The beam was meshed into 30 nodes which we determined to be appropriate as the output variance was negligible for a higher number of nodes.

We assessed the wings von Mises stress and the vertical deflection for both in flight and on-ground conditions. Notably, we compared the max calculated stress to the yield stress of the material. A safety factor less than 2 did not meet the design requirements. Similarly, a deflection of greater than 1 meter in the case of the on-ground condition also did not meet the design requirements.

TABLE C: A summary of the results for the static analysis. Considering both with lift and without lift conditions. In SI Units (see Appendix D).

The displacement values for the no lift condition do not exceed or equal

Property	2412 7075	4412 7075	2412 304	4412 304
Stress [No Lift]	6.80 E+07	7.03 E+07	1.22 E+08	1.26 E+08
Disp [No Lift]	1.76 E-01	1.67 E-01	1.36 E-01	1.29 E-01
Stress [Lift]	7.31 E+07	7.53 E+07	2.60 E+09	2.69 E+09
Disp [Lift]	3.25 E-01	3.08 E-01	3.46 E+00	3.278 E+00

1m and so fit the design requirements.

Regarding the stress values, we compared the values to the yield stress of the material.

TABLE D: Calculations of the safety factor. The yield stress value for each material is divided by the stress value. Yellow cells do not meet the design requirements (see Appendix E).

Property	2412 7075	4412 7075	2412 304	4412 304
Stress [No Lift]	6.80 E+07	7.03 E+07	1.22 E+08	1.26 E+08
SF [No Lift]	6.32	6.12	1.76	1.71
Stress [Lift]	7.31 E+07	7.53 E+07	2.60 E+09	2.69 E+09
SF [Lift]	5.88	5.71	0.08	0.08

From **Table D** in the current configuration the steel-based designs are less capable of resisting the stresses prevalent in wing structures this is especially true during flight loading conditions.

Dynamic Vibration Analysis

When considering the vibrational response of the structures, we represented the wing with the same configuration we employed for the static analysis. We reduced the loading to just fuel and the mass properties of the structure.

The fuel was represented as an inertial mass applied at a point 400 mm from the root.

The number of nodes was also left at 30. However, the number of nodes has no noticeable effect on the output for vibrational analysis and so could just as easily have been done accurately with 1 node.

This was verified in the testing before getting further results.

TABLE E: A summary of the results for the static analysis. Considering both with lift and without lift conditions. In Hertz (see Appendix F).

Property	2412 7075	4412 7075	2412 304	4412 304
Mode 1 [Fuel]	1.774	1.8189	1.8202	1.8666
Mode 2 [Fuel]	6.0282	6.1377	7.9991	8.1409
Mode 3 [Fuel]	11.165	11.008	11.621	11.482
Mode 1 [No Fuel]	1.9089	1.9576	1.8681	1.9158
Mode 2 [No Fuel]	11.255	11.337	11.039	11.127
Mode 3 [No Fuel]	12.321	12.295	12.058	12.034

The vibrational analysis shows that all the first mode value are well below 16 Hz (20% below 20 Hz). This meets the design requirements and indicates that the wing structures should not resonate with the engines during idle.

It also shows that the first mode for both fueled and un-fueled structures is relatively similar whereas the second mode deviates rather substantially.

Contour Plots

The relevant contour plots as produced by Abacus CAE (See appendix G – E for plots of stress and displacement).

Conclusion

Modern computing technology's, specifically Finite Element Analysis can allow for the creation of more refined and efficient designs with substantially less work required. When compared to the undertaking that went into designing the U-2 aircraft FEM can cut down on prototyping and the need to create expensive scale models. This is a large advantage for companies evaluating many designs and means that more designs can be tested and considered. Regarding the materials explored above clearly steel is not ideal as a skin material especially due to its high density but with some amendments and refinements steel could still serve as a functional skin and is employable for other aircraft structural elements. Further, regarding aluminum, the thickness certainly could have been reduced to bring down the overall weight. This is evidenced by the large safety factors evaluated in **Table D**. So, technologies like FEM specifically implementations of FEM like Abacus CAE are clearly valuable tools to refine structures and evaluate their validity.

References

Bibliography

[1]
"304 Stainless Steel | Grade 304," *www.australwright.com.au*. https://www.australwright.com.au/technical-data/alloys/stainless-steel/304-stainless-steel/

[2]
Wikipedia Contributors, "7075 aluminium alloy," *Wikipedia*, Sep. 20, 2019. https://en.wikipedia.org/wiki/7075_aluminium_alloy

[3]
"ASM Material Data Sheet," *asm.matweb.com*. https://asm.matweb.com/search/SpecificMaterial.asp?bassnum=mq304a

[4]
"Airfoil plotter," *airfoiltools.com*. http://airfoiltools.com/plotter/index

[5]
Ira Herbert Abbott and A. Edward, *Theory of wing sections, including a summary of airfoil data, by Ira H. Abbott and Albert E. von Doenhoff.* New York Dover Publications, 1959.

[6]
M. H. Sadraey, *Aircraft design : a systems engineering approach*. Chichester: John Wiley & Sons, 2013.

Appendices

Appendix A - Summary of the materials and their relevant properties.

Material	*Aluminum 7075-T6*	*SAE 304 Stainless Steel*	*Units*
Density	2810	7900	kg/m^3
Youngs Modulus	71.7	193	MPa
Poisson's Ratio	0.33	0.3	
Yield Stress	430	215	MPa

Appendix B - Summary of the wing weight and the loading conditions for each case.

Airfoil	*2412*		*4412*	
Material	SAE 304 Stainless Steel	Aluminum 7075-T6	SAE 304 Stainless Steel	Aluminum 7075-T6
Mass [kg]	6775	2410	6796	2417
Wing Weight [N]	66462.75	23642.1	66668.76	23710.77
Fuel Weight [N]	53400.735	53400.735	53400.735	53400.735
Lift Force [N]	112638	112638	155459	155459

Appendix C - Maximum lift coefficient versus ideal lift coefficient for several NACA airfoil sections.

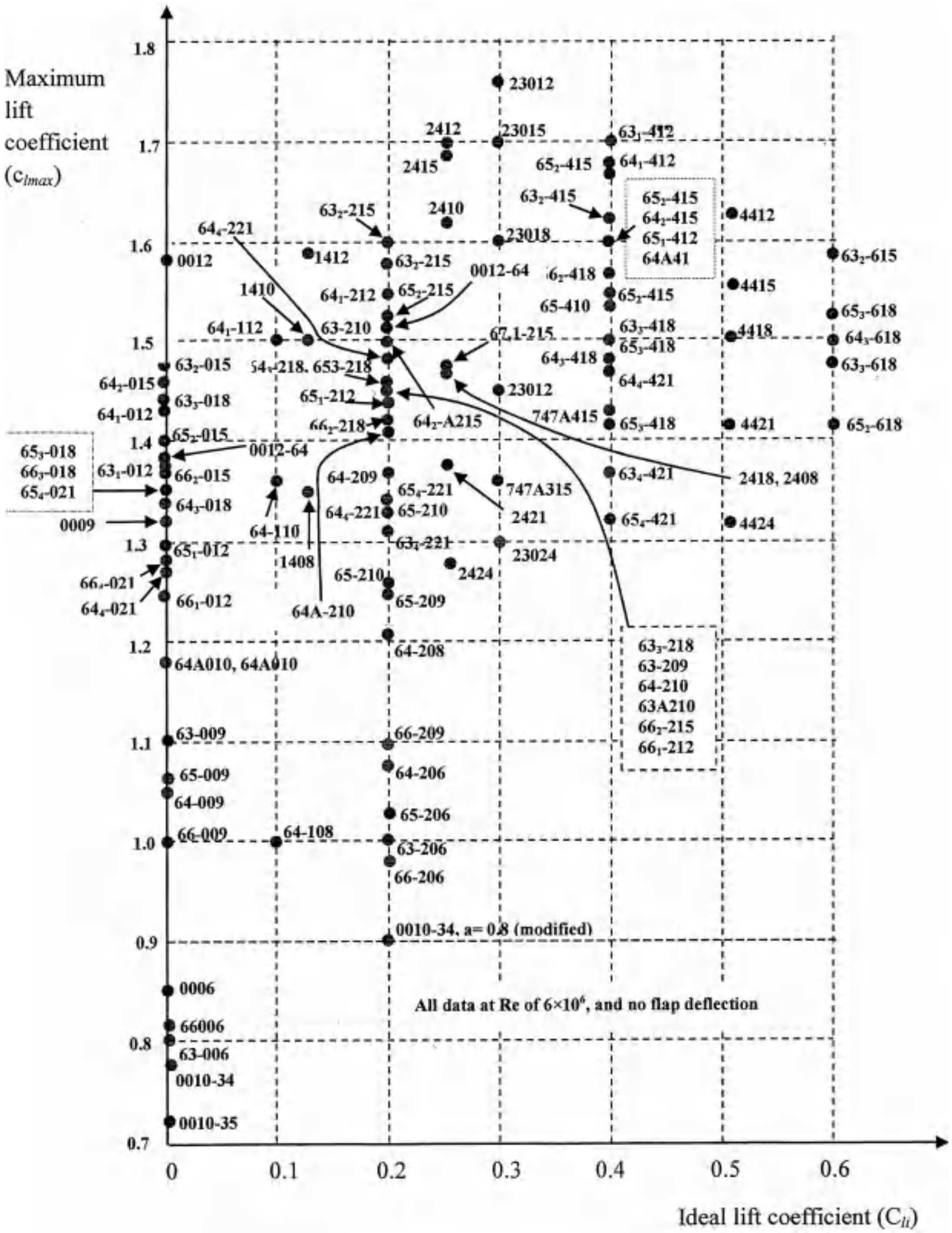

Appendix D - A summary of the results for the static analysis. Considering both with lift and without lift conditions.

Value	*NACA 2412 [7075]*	*NACA 4412 [7075]*	*NACA 2412 [304]*	*NACA 4412 [304]*
Max-Stress [No Lift] [Pa]	6.80E+07	7.03E+07	1.22E+08	1.26E+08
Max-Displacment [Tip] [No Lift] [m]	1.76E-01	1.67E-01	1.36E-01	1.29E-01
Max-Stress [Lift] [Pa]	7.31E+07	7.53E+07	2.60E+09	2.69E+09
Max-Displacment [Tip] [Lift] [m]	3.25E-01	3.08E-01	3.46	3.278

Appendix E - Calculations of the safety factor. The yield stress value for each material is divided by the stress value. Yellow cells do not meet the design requirements.

Value	*NACA 2412 [7075]*	*NACA 4412 [7075]*	*NACA 2412 [304]*	*NACA 4412 [304]*
Max-Stress [No Lift] [Pa]	6.80E+07	7.03E+07	1.22E+08	1.26E+08
Safety Factor [No Lift]	6.32	6.12	1.76	1.71
Max-Stress [Lift] [Pa]	7.31E+07	7.53E+07	2.60E+09	2.69E+09
Safety Factor [Lift]	5.88	5.71	0.08	0.08

Appendix F - A summary of the results for the static analysis. Considering both with lift and without lift conditions.

Value	*NACA 2412 [7075]*	*NACA 4412 [7075]*	*NACA 2412 [304]*	*NACA 4412 [304]*
Mode 1 [Fuel] [Hz]	1.774	1.8189	1.8202	1.8666
Mode 2 [Fuel] [Hz]	6.0282	6.1377	7.9991	8.1409
Mode 3 [Fuel] [Hz]	11.165	11.008	11.621	11.482
Mode 1 [No Fuel] [Hz]	1.9089	1.9576	1.8681	1.9158
Mode 2 [No Fuel] [Hz]	11.255	11.337	11.039	11.127
Mode 3 [No Fuel] [Hz]	12.321	12.295	12.058	12.034

Appendix G – Contour plots for **lift** loading conditions

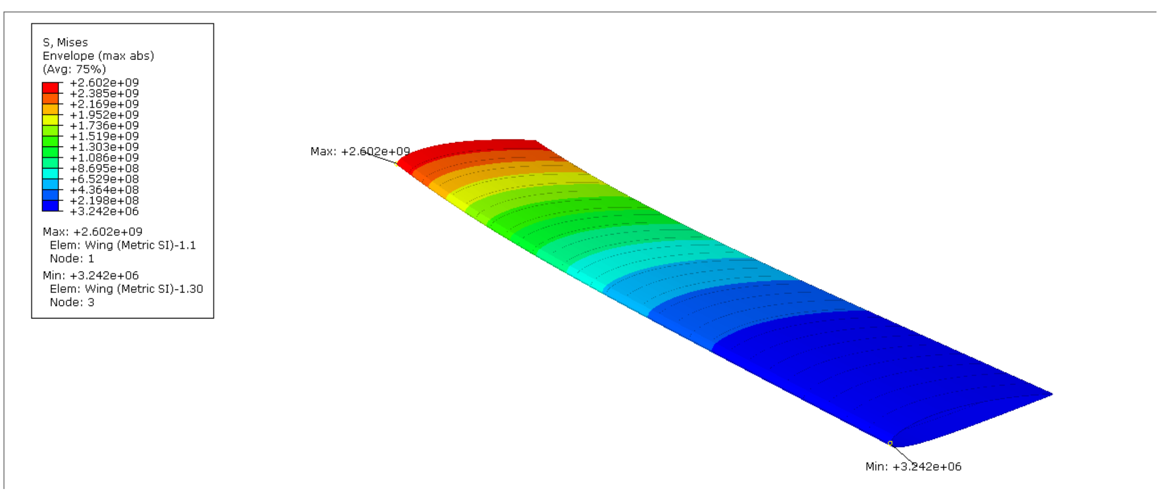

Figure G1: von Mises stress contour plot for 304 Steel with NACA 2412 Airfoil

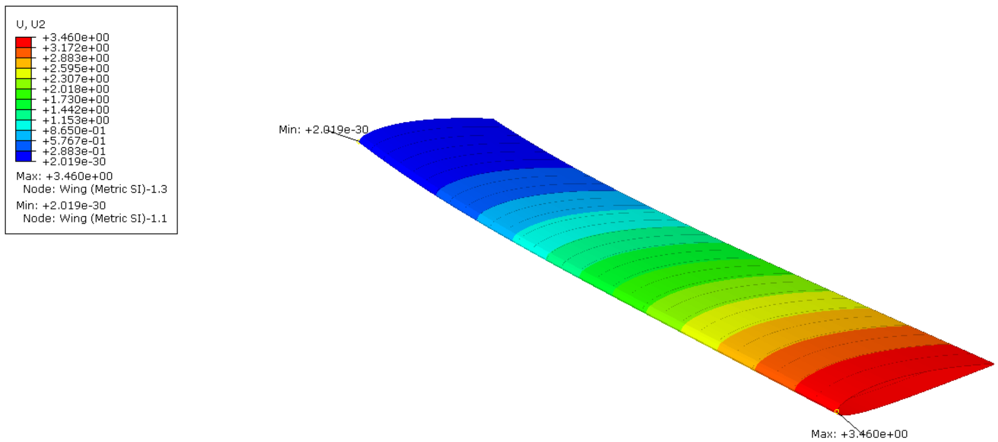

Figure G2: Displacement contour plot for 304 Steel with NACA 2412 Airfoil

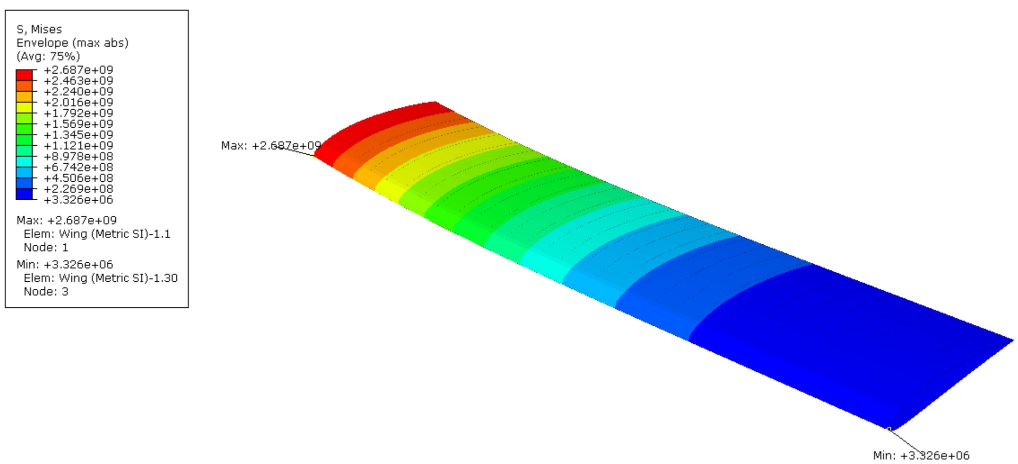

Figure G3: von Mises stress contour plot for 304 Steel with NACA 4412 Airfoil

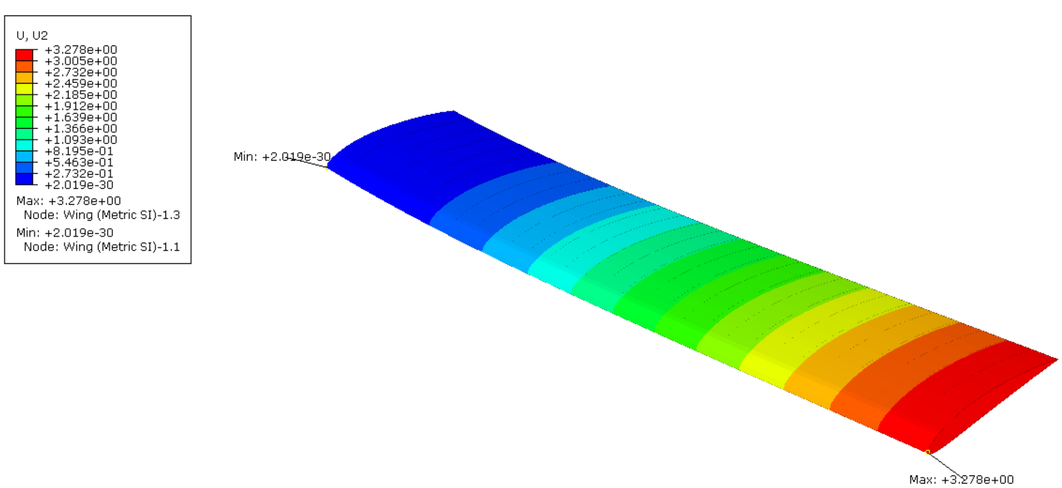

Figure G4: Displacement contour plot for 304 Steel with NACA 4412

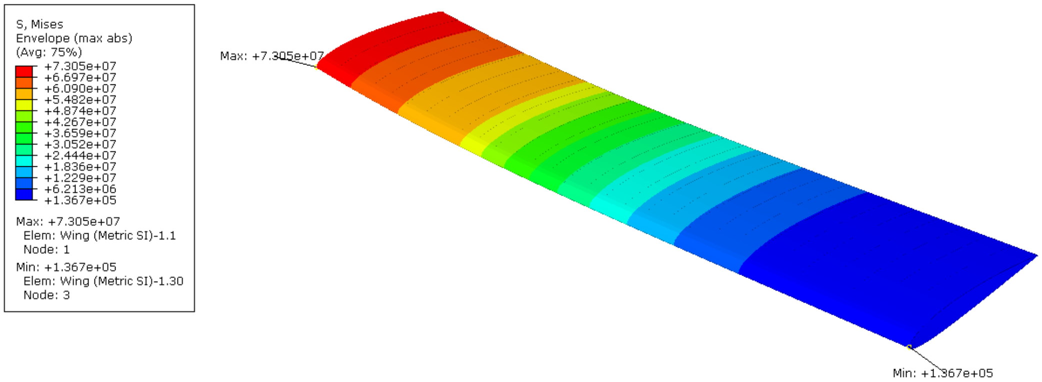

Figure G5: von Mises stress contour plot for 7075 Aluminum with NACA 2412 Airfoil

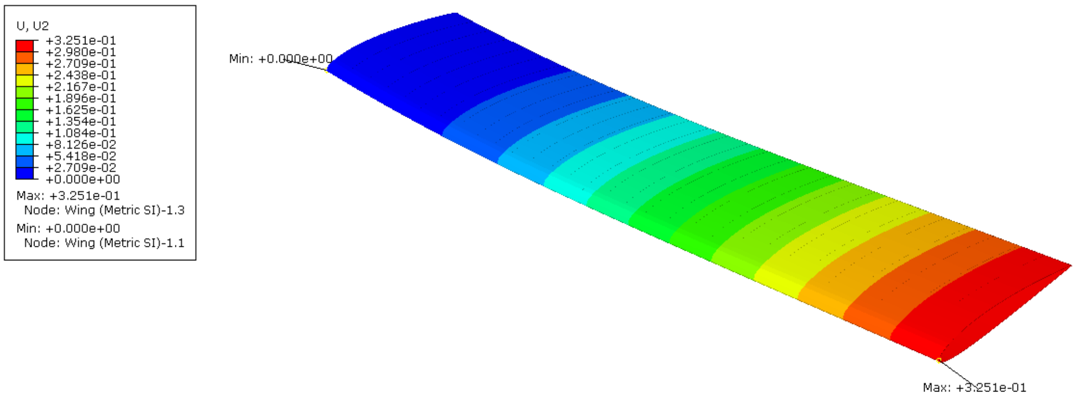

Figure G6: Displacement contour plot for 7075 Aluminum with NACA 2412 Airfoil

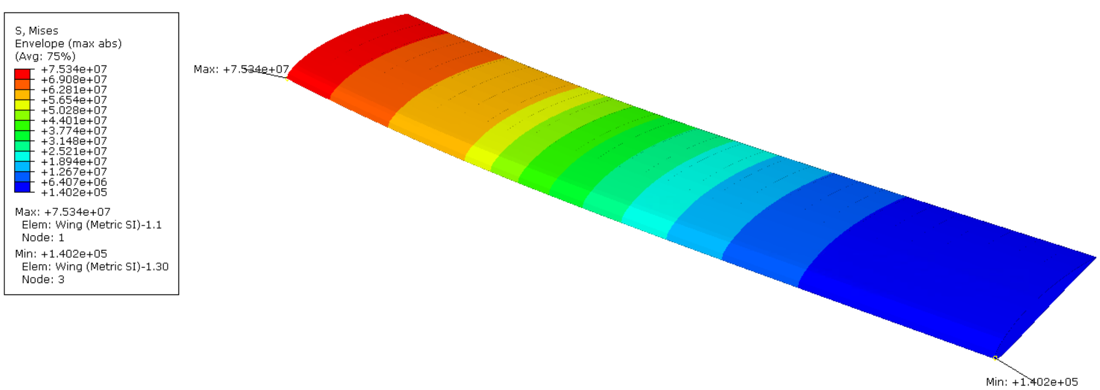

Figure G7: von Mises stress contour plot for 7075 Aluminum with NACA 4412 Airfoil

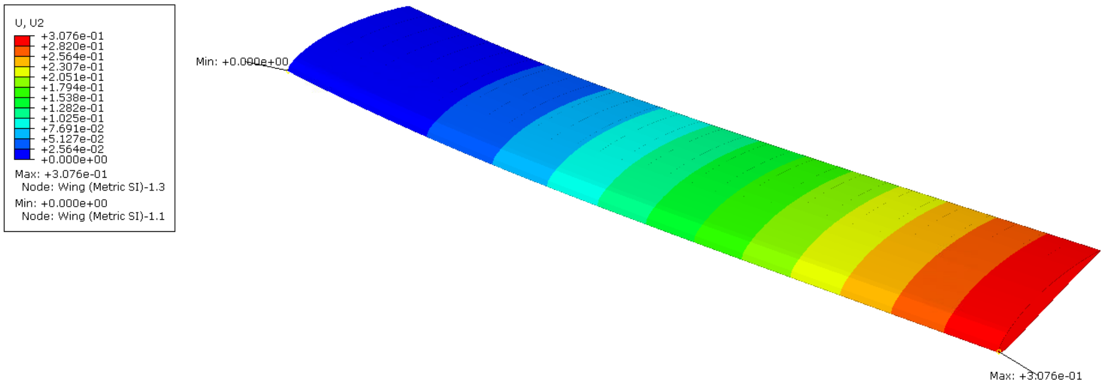

Figure G8: Displacement contour plot for 7075 Aluminum with NACA 4412 Airfoil

Appendix E – Contour plots for **no lift** loading conditions

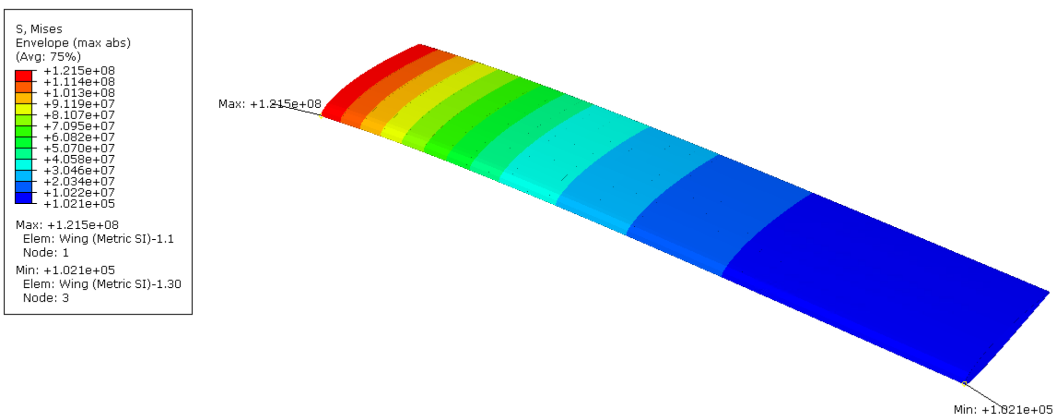

Figure E1: von Mises stress contour plot for 304 Steel with NACA 2412 Airfoil

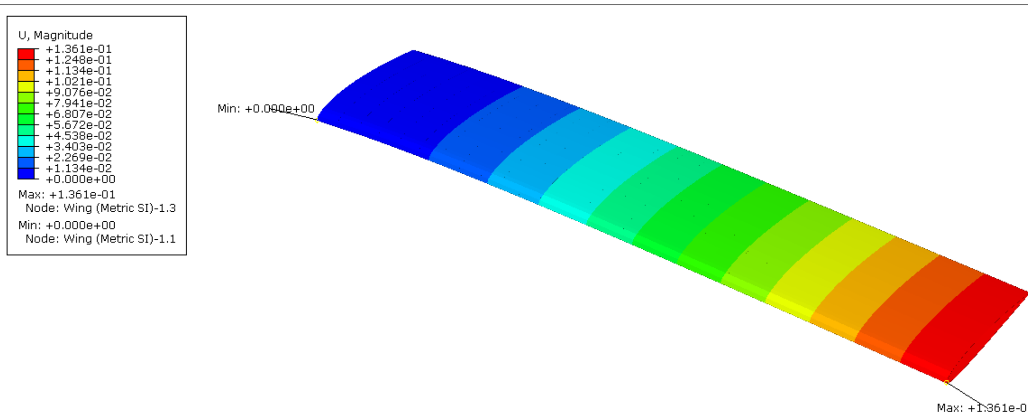

Figure E2: Displacement contour plot for 304 Steel with NACA 2412 Airfoil

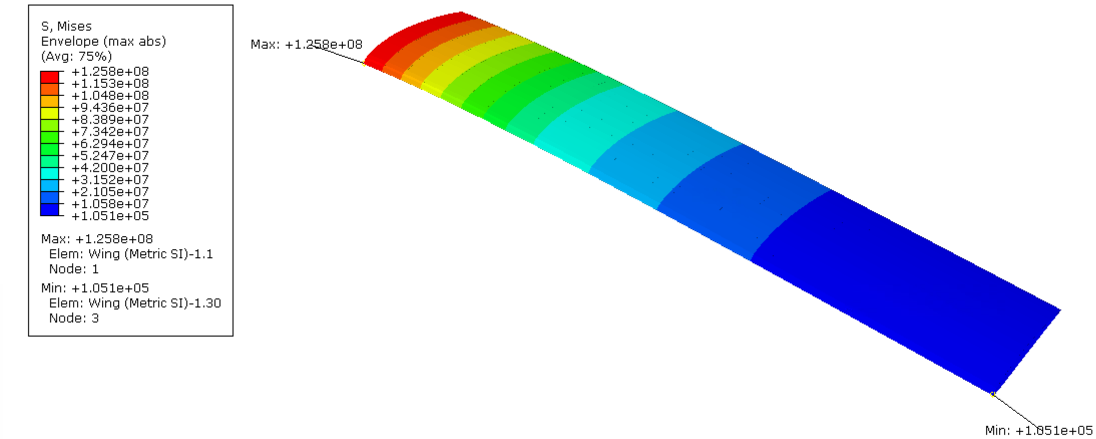

Figure E3: von Mises stress contour plot for 304 Steel with NACA 4412 Airfoil

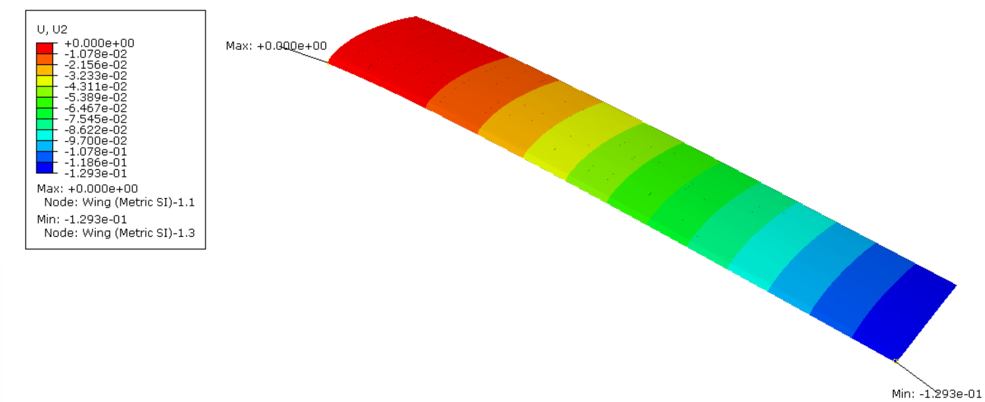

Figure E4: Displacement contour plot for 304 Steel with NACA 4412 Airfoil

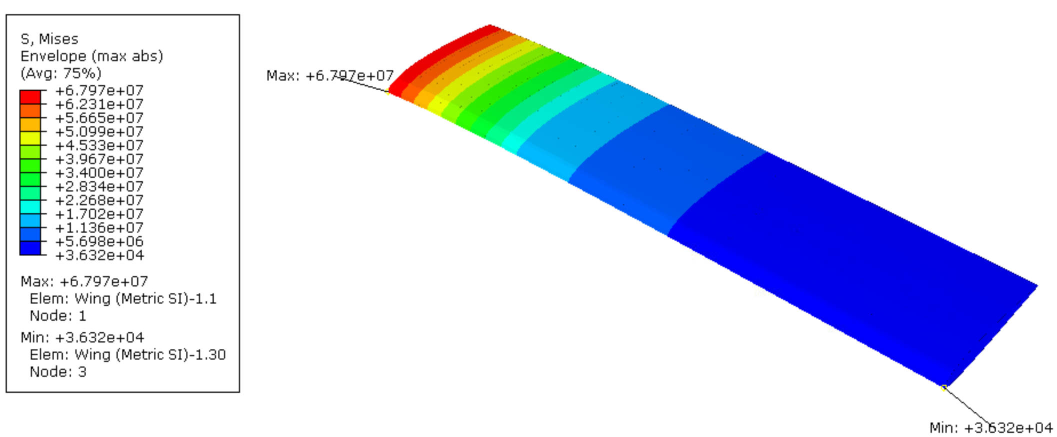

Figure E5: von Mises stress contour plot for 7075 Aluminum with NACA 2412 Airfoil

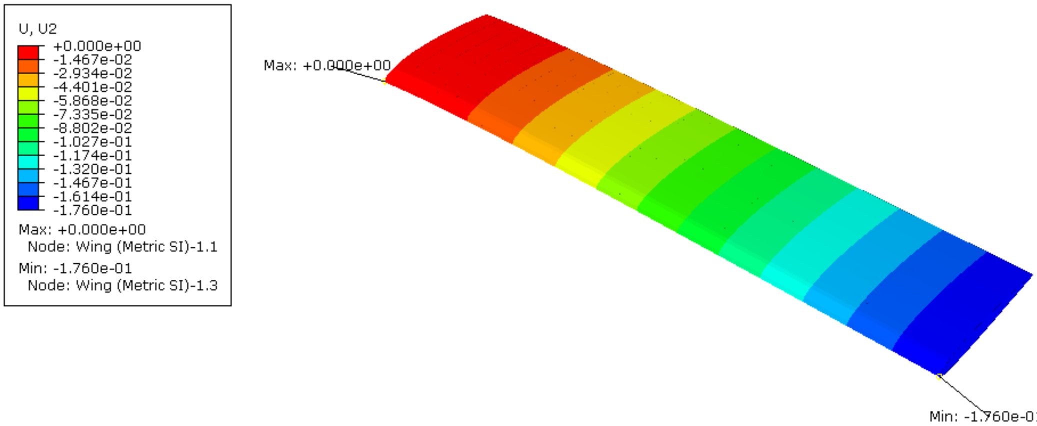

Figure E6: Displacement contour plot for 7075 Aluminum with NACA 2412 Airfoil

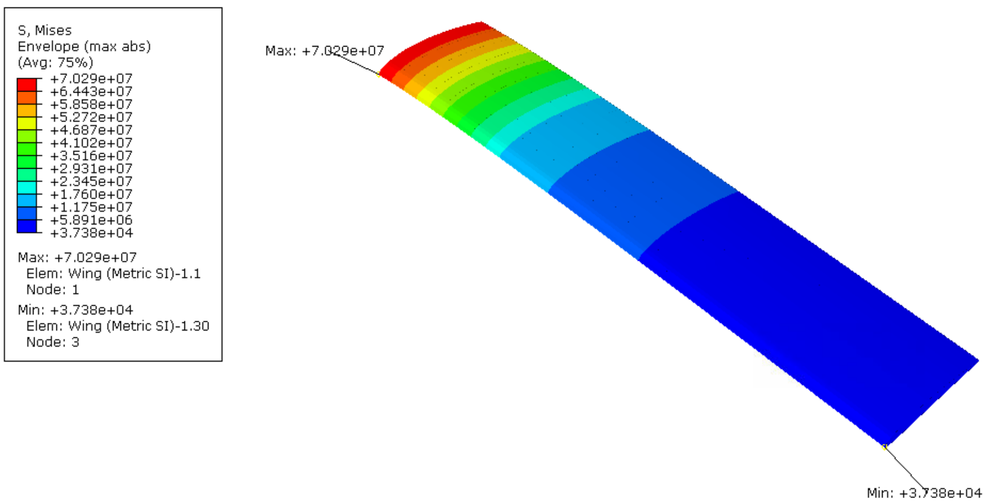

Figure E7: von Mises stress contour plot for 7075 Aluminum with NACA 4412 Airfoil

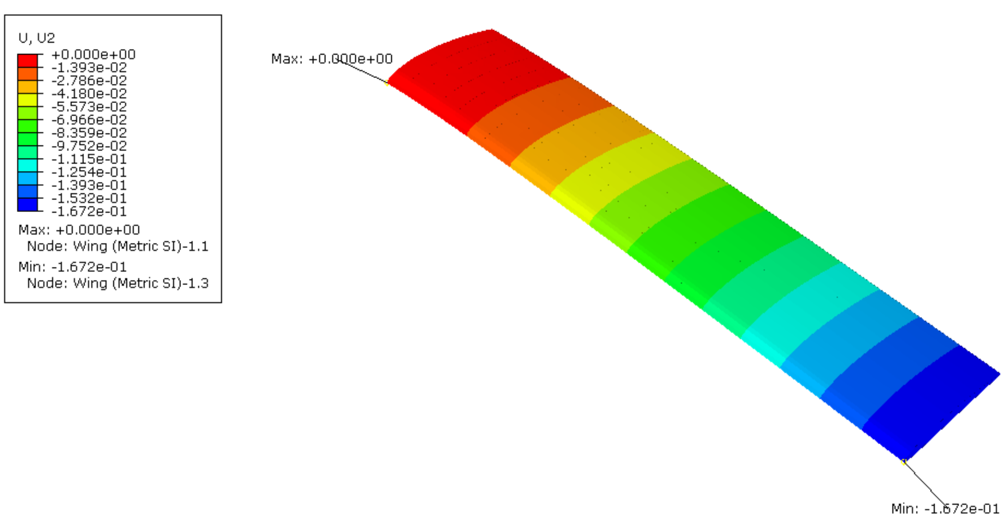

Figure E8: Displacement contour plot for 7075 Aluminum with NACA 4412 Airfoil